Flame," *Experimental Fluids,* Vol. 3, 1985, pp. 323-339.
[11]Driscoll, J. F., Schefer, R. W., and Dibble, R. W., "Mass Fluxes $\overline{\rho' u'}$, and $\overline{\rho' v'}$, measured in a Turbulent Nonpremixed Flame," *Proceedings of the Nineteenth Symposium (International) on Combustion,* The Combustion Inst., Pittsburgh, PA, 1982, pp. 477-485.
[12]Zhu, J. Y., So, R. M. C., and Otugen, M. V., "Turbulent Mass Flux Measurements Using a Laser/Hot-Wire Technique," *International Journal of Heat and Mass Transfer,* Vol. 31, 1988, pp. 819-829.
[13]Stevenson, W. H., Thompson, H. D., and Roesder, T. C., "Direct Measurement of Laser Velocimeter Bias Errors in a Turbulent Flow, *AIAA Journal,* Vol. 20, 1982, pp. 1720-1723.
[14]So, R. M. C. and Liu, T. M., "On Self-Preserving, Variable-Density Turbulent Free Jets," *Zeitschrift für angewandte Mathematik und Physik,* Vol. 37, 1986, pp. 538-558.

Unsteady Transition Location

Kenneth F. Stetson*
Air Force Wright Aeronautical Laboratories, Wright-Patterson Air Force Base, Ohio

Nomenclature

h	= local heat transfer coefficient (recovery temperature of 0.9 T_0 assumed, Btu/ft^2-s °R)
k	= roughness height, cm (in.)
p	= pressure, k Pa (lb/in.^{2})
R	= radius, cm (in.)
Re	= Reynolds number
Re_{x_T}	= transition Reynolds number based upon conditions at the edge of the boundary layer and the surface distance from the stagnation point to the location of transition
Re_Θ	= Reynolds number based upon conditions at the edge of the boundary layer and the laminar boundary-layer momentum thickness
t	= time, s
T	= temperature, °K(°R)
X	= surface distance, cm (in.)
Θ	= laminar boundary-layer momentum thickness, cm (in.)

Subscripts

ad	= adiabatic
B	= base
e	= edge of boundary layer
N	= nose
w	= wall
∞	= freestream

Received Oct. 20, 1987. This paper is declared a work of the U.S. Government and is not subject to copyright protection in the United States.

*Aerospace Engineer, High Speed Aero Performance Branch, Aeromechanics Division, Flight Dynamics Laboratory. Associate Fellow AIAA.

Introduction

THE movement of boundary-layer transition on a wind tunnel model, while the freestream conditions remain constant, is an old topic, yet one that is not well understood. The stability theory of Lees[1] indicated that wall cooling had a stabilizing effect on a laminar boundary layer at supersonic Mach numbers. Van Driest[2] made calculations that indicated after a certain cooling temperature ratio was exceeded, the boundary layer remained laminar for any Reynolds number. Subsequently, wind tunnel experiments were performed to check the validity of these theoretical predictions. The early wind tunnel investigations of the effect of wall cooling on boundary-layer transition found, as predicted by theory, that decreasing the model surface temperature increased the transition Reynolds number. However, when liquid nitrogen was used to obtain additional surface cooling, an unexpected event occurred[3]: The stabilizing trend was reversed and the transition Reynolds number decreased with further reductions in surface temperature. There were two branches of the Re_{x_T} vs T_w/T_{ad} curve: The upper branch followed the trend of theory and suggested that the laminar boundary layer would be completely stabilized for temperature ratios below about 0.5; the lower branch showed an adverse effect of surface cooling that has never been explained (called transition reversal). Transition reversal was observed for several configurations, both with and without surface roughness. Surface roughness was not believed to provide a suitable answer for the observed results.

Muir and Trujillo[4] reported an unsteady transition location on their blunt 8-deg half-angle cone tested at Mach 6. They observed that for the 32% blunt nosetip ($R_N/R_B = 0.32$), transition moved rearward with time, similar to the blunt configurations of Ref. 3. It was noted that this phenomenon occurred only with the large nosetip bluntness, and for the sharper configurations, which were subjected to the same environment and experienced similar increases in wall temperature, the transition location remained unchanged with time.

During the course of a more recent wind tunnel investigation of the effects of nosetip bluntness on boundary-layer transition, some transition movement with time results were also obtained.[5-7] These new results do not provide an explanation for the transition-reversal phenomenon, but they do provide a better understanding of why transition can be unsteady on some blunt configurations.

Results and Discussion

The experiments were conducted in the Flight Dynamics Laboratory Mach 6 wind tunnel. This tunnel is a blow-down facility operating at a reservoir temperature of 611 K (1100°R) and a reservoir pressure range of 4827 to 14,480 k Pa (700 to 2100 psia), corresponding to a unit Reynolds number range of 31.8×10^6 to 99.4×10^6/m (9.7×10^6 to 30.3×10^6/ft). The test core of approximately 25.4 cm (10 in.) is produced by a contoured axisymmetric nozzle with a physical exit diameter of 31.2 cm (12.3 in.). Additional details of the wind tunnel can be found in Ref. 8. The test model was a thin-skin, 8-deg half-angle cone containing two rays of thermocouples and had a base diameter of 10.2 cm (4 in.). The location of boundary-layer transition was obtained from heat-transfer measurements. Heat-transfer rates were caluclated from the increase in the wall temperature of the model, using standard thin-skin data reduction techniques.

Transition experiments of Ref. 7 found low transition Reynolds numbers associated with the initial portion of a cone frustum; i.e., for several nose radii downstream from the nosetip, in spite of the existence of a favorable pressure gradient (designated as early frustum transition). It was determined that nosetip instabilities were responsible for these low transition Reynolds numbers and that the occurrence of transition in this region could be related to some threshold value of nosetip Reynolds number and nosetip roughness. This was the

same transition criteria that was applied to nosetip transition studies and resulted in the PANT correlation.[9] Therefore, it was considered of interest to look at the early frustum transition data in terms of the PANT nosetip parameters. Figure 1 contains the results. All of the parameters are evaluated at the sonic point. The results of the PANT program[9] and Demetriades[10] are shown to indicate the conditions that produce transition on the nosetip. The data points shown are the nosetip conditions that correspond to the threshold of early frustum transition. The points shown with an arrow indicate that the critical conditions were not obtained, and the direction of the arrow indicates the direction to the threshold condition. Several characteristics of early frustum transition differed from other frustum transition data.[7] An interesting feature of the nosetip-instability-dominated frustum transition data was that generally the transition location was a unsteady. (A number of checks on the steadiness of transition location when "normal" frustum transition occured found no evidence of unsteadiness.) In a number of tests, transition location vs time data were obtained and the transition location was always found to move downstream with time, varying in the amount and the rapidity of movement. It appeared as though the greatest movement occurred with a choice of nosetip conditions corresponding to a location near the threshold line identifying the nosetip-instability-dominated region. Moving farther above the threshold line produced slower transition movement and a more limited change. It was not possible to investigate this aspect of transition more fully because of the limitations of the operating conditions of the wind tunnel and maximum nosetip size.

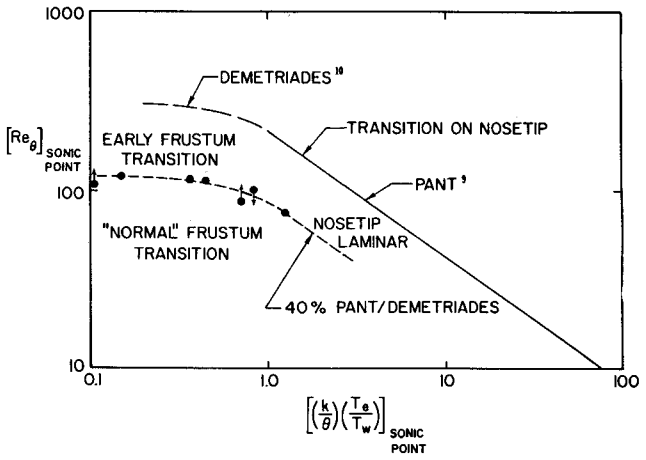

Fig. 1 Nosetip instability effects on cone frustum transition.

To demonstrate the sensitivity of early frustum transition to nosetip conditions, one side of the 30% blunt nosetip was roughened to approximately 50 μ-in. (rms) and the other side was left smooth. The tip was oriented such that one ray of frustum thermocouples would be behind the rough side of the nosetip and the other ray of frustum thermocouples would be behind the smooth side of the nosetip. The test conditions were selected such that the nosetip parameters on the rough side of the nosetip corresponded closely to the threshold line of Fig. 1 and the smooth side of the nosetip was just below the line. The results are shown in Fig. 2. The heat-transfer rate results shown with circles represent the ray behind the smooth portion of the nosetip and indicate a completely laminar boundary layer. The local length Reynolds number at the end of the model was approximately 4.6×10^6, thus the transition Reynolds number was at some unknown larger value. The results shown with squares represent the ray behind the por-

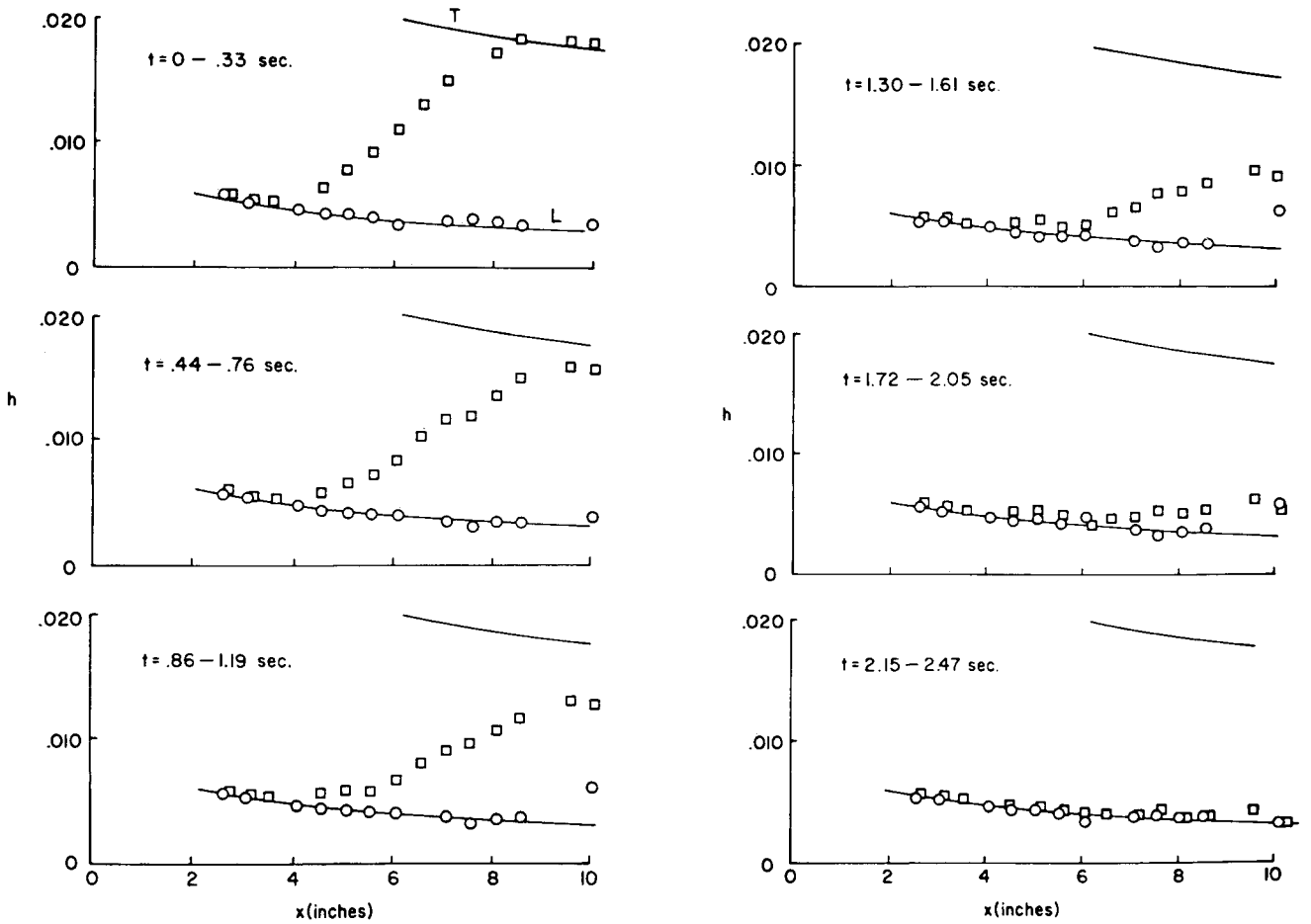

Fig. 2 An example of unsteady transition location data.

tion of the nosetip with 50 μ-in. roughness and indicate that transition had occurred at a Reynolds number of approximately 1.8×10^6. These results provide additional evidence of nosetip threshold conditions that determine when the nosetip would produce low frustum transition Reynolds numbers. This example also illustrates a case of unsteady transition location for this early frustum transition condition. Transition steadily moved rearward with increasing time and in 2.5 s both sides of the model had a completely laminar boundary layer. (The time interval for each sequence of data is indicated. As shown, $t=0$ is the time when the model arrived at the tunnel centerline.)

It was interesting to relate the transition reversal results of Refs. 3 and 4 to these present findings. An estimate of the sonic point conditions for the experiments of both references indicated they were close to the threshold conditions for the case of nosetip-instability-dominated frustum transition. This suggests the possibility that these transition data were not really a transition reversal resulting from frustum surface temperature changes, but may have resulted from nosetip instabilities.

References

[1]Lees, L., "The Stability of the Laminar Boundary Layer in a Compressible Fluid," NACA Rept. 876, 1947.

[2]Van Driest, E. R., "Calculations of the Stability of the Laminar Boundary Layer in a Compressible Fluid on a Flat Plate With Heat Transfer," *Journal of Aeronautical Sciences,* Vol. 19, Dec. 1952, pp. 801–812, 828.

[3]Jack, J. R., Wisniewski, R. J., and Diaconis, N. S., "Effect of Extreme Surface Cooling on Boundary Layer Transition," NACA TN-4094, Oct. 1957.

[4]Muir, J. R. and Trujillo, A. A., "Experimental Investigation of the Effects of Nose Bluntness, Free-Stream Unit Reynolds Number, and Angle of Attack on Cone Boundary Layer Transition at a Mach Number of 6," AIAA Paper 72-216, Jan. 1972.

[5]Stetson, K. F., "Effect of Bluntness and Angle of Attack on Boundary Layer Transition on Cones and Biconic Configurations," AIAA Paper 79-0269, Jan. 1979.

[6]Stetson, K. F., "Hypersonic Boundary Layer Transition Experiments," AFWAL-TR-80-3062, Oct. 1980.

[7]Stetson, K. F., "Nosetip Bluntness Effects on Cone Frustum Boundary Layer Transition in Hypersonic Flow," AIAA Paper 83-1763, July 1983.

[8]Fiore, A. W. and Law, C. H., "Aerodynamic Calibration of the Aerospace Research Laboratories M=6 High Reynolds Number Facility," ARL-TR-75-0028, Feb. 1975.

[9]Anderson, A. D., "Interim Report, Passive Nosetip Technology (PANT) Program, Vol. X, Appendix, Boundary Layer Transition on Nosetips With Rough Surfaces," Space and Missile Systems Organization, SAMSO-TR-74-86, Jan. 1975.

[10]Demetriades, A., "Nosetip Transition Experimentation Program, Final Report, Vol.2," Space and Missile Systems Organization, SAMSO-TR-76-120, July 1977.

Effects of Transverse Curvature on Oscillatory Flow Along a Circular Cylinder

Y. T. Chew*
National University of Singapore, Singapore
and
C. Y. Liu†
Nanyang Technological Institute, Singapore

Received Oct. 22, 1987; revision received Feb. 19, 1988.

*Associate Professor, Department of Mechanical and Production Engineering. Member AIAA.

†Professor, School of Mechanical and Production Engineering. Member AIAA.

Introduction

OSCILLATORY flows with zero mean velocity can be found in a variety of natural phenomena. The classic example of oscillatory flows in unbounded stagnant fluid is that over an infinite flat plate executing periodic sinusoidal motion along its plane. This was solved by Stokes[1] and is often referred to in the literature as Stokes flow. Some characteristic features of this flow are that, although the flow oscillates at the same frequency as the plate, it lags behind the plate, and the phase lag is proportional to the distance from the plate. The layer of oscillatory flow also is referred to in the literature as "Stokes layer."[2] Although there are not many engineering problems that can be classified as Stokes flow, it should be noted that Stokes layers can be embedded in other flowfields with almost independent properties. An example of this is in unsteady laminar boundary-layer flow. Lighthill[3] found mathematically that at large frequency of unsteadiness, a Stokes layer with profiles independent of the profiles of the steady layer is generated. Unsteady laminar boundary-layer flow has engineering application in the design of turbine and compressor blades where the flow along the blade is subjected to disturbances caused by the wake of preceding row of blades.

In the present Note, a general oscillatory Stokes flow including the transverse curvature effect is presented.

Analysis

It is assumed that a circular cylinder of radius a is of infinite length and oscillates azimuthally in a stationary, unbounded, incompressible Newtonian fluid. The equation of motion in cylindrical coordinates can be reduced to

$$\frac{\partial u}{\partial t}=\nu\left(\frac{\partial^2 u}{\partial r^2}+\frac{1}{r}\frac{\partial u}{\partial r}\right) \tag{1}$$

and the boundary conditions are

$$r=a,\ u=U_0\cos\omega t \quad \text{and} \quad r=\infty,\ u=0$$

where ν is the kinematic viscosity and ω the angular frequency.

Equation (1) is a linear, second-order partial differential equation. It can be solved by separation of variables. Assuming

$$u(r,t)=P(r)Q(t) \tag{2}$$

the solutions of functions Q and P are

$$Q=Ae^{i\omega t} \tag{3}$$

$$P=BI_0(\sqrt{i\omega/\nu}\,r)+CK_0(\sqrt{i\omega/\nu}\,r) \tag{4}$$

where A, B, and C are constants, I_0 and K_0 are modified zero-order Bessel function of first and second kind, respectively. The function I_0 does not converge when $r\to\infty$; thus, B must be equal to zero in order to satisfy the boundary condition.

The solution of Eq. (1) subjected to the boundary conditions can then be written as

$$u(r,t)=U_0\left[\frac{\mathrm{ker}_0(ka)\mathrm{ker}_0(kr)+\mathrm{kei}_0(ka)\mathrm{kei}_0(kr)}{\mathrm{ker}_0^2(ka)+\mathrm{kei}_0^2(ka)}\cos\omega t\right.$$

$$\left.+\frac{\mathrm{kei}_0(ka)\mathrm{ker}_0(kr)-\mathrm{ker}_0(ka)\mathrm{kei}_0(kr)}{\mathrm{ker}_0^2(ka)+\mathrm{kei}_0^2(ka)}\sin\omega t\right] \tag{5}$$